

# Interactive 3-dimensional visualization tools for stereotactic atlas-based functional neurosurgery

Philippe St-Jean <sup>$\alpha\beta$</sup> , Reza Kasrai <sup>$\alpha\pi$</sup> , Diego Clonda <sup>$\alpha\beta$</sup> ,  
Abbas F. Sadikot <sup>$\phi$</sup> , Alan C. Evans <sup>$\alpha\beta\pi\phi$</sup> , and Terry M. Peters <sup>$\alpha\beta\pi\phi$</sup>

<sup>$\alpha$</sup> McConnell Brain Imaging Center and  <sup>$\phi$</sup> Department of Neurology and Neurosurgery,  
Montreal Neurological Institute and Hospital,

<sup>$\pi$</sup> Department of Biomedical Engineering and  <sup>$\beta$</sup> Medical Physics Unit,  
McGill University, Montréal, QC, Canada

## ABSTRACT

Many of the critical basal ganglia structures are not distinguishable on anatomical magnetic resonance imaging (MRI) scans, even though they differ in functionality. In order to provide the neurosurgeon with this missing information, a deformable volumetric atlas of the basal ganglia has been created from the Shaltenbrand and Wahren atlas of cryogenic slices. The volumetric atlas can be non-linearly deformed to an individual patient's MRI. To facilitate the clinical use of the atlas, a visualization platform has been developed for pre- and intra-operative use which permits manipulation of the merged atlas and MRI data sets in two- and three-dimensional views. The platform includes graphical tools which allow the visualization of projections of the leukotome and other surgical tools with respect to the atlas data, as well as pre-registered images from any other imaging modality. In addition, a graphical interface has been designed to create custom virtual lesions using computer models of neurosurgical tools for intra-operative planning. To date 17 clinical cases have been successfully performed using the described system.

**Keywords:** image-guided neurosurgery, atlas-based guidance, 3D visualization, thalamus, Parkinson's syndrome, movement disorders

## 1. INTRODUCTION

### 1.1 Clinical motivation

Symptomatic Parkinson's syndrome manifests itself in a variety of ways including tremor, rigidity, bradykinesia, and impaired gait. Most of these symptoms can be relieved by the prescription of the drug L-dopa, except for tremors, which are more resistant to the drug. In some patients however, the tremors are made even worse with L-dopa. Parkinsonian patients suffering from significant tremors, and those who have gained only a mild improvement (or no improvement at all) of their general state from L-dopa can benefit from surgery. Pallidotomies are usually performed when the patient suffers from rigidity more than from tremors, whereas thalamotomies are performed to alleviate tremors. The probability of relief of symptoms for these candidates is around 80%<sup>1</sup>. Currently at the Montreal Neurological Institute and Hospital (MNI/H), the target for thalamotomy is the nucleus ventralis intermedialis (Vim) in the thalamus, while the target for pallidotomy is part of the globus pallidus medialis (Gpm).

---

Address correspondence to:

Terry M. Peters, Imaging Research Laboratory, Robarts Research Institute, 100 Perth Drive, London, ON, N6A 5K8, Canada;  
Telephone: (519) 663-5777 (X4159); Fax: (519) 663-3403; e-mail: tpeters@irus.rrri.uwo.ca;  
Web: [http://www.bic.mni.mcgill.ca/research\\_groups/igns/](http://www.bic.mni.mcgill.ca/research_groups/igns/)

Other authors:

stjean@crm.umontreal.ca, rkasrai@bic.mni.mcgill.ca, clonda@crm.umontreal.ca, sadikot@nil.mni.mcgill.ca, alan@bic.mni.mcgill.ca.

## 1.2 The stereotactic frame

Since these operations involve deep-brain structures, they require the use of a stereotactic frame attached to the patient's head. An arc system is mounted on the frame to support neurosurgical tools (Figure 1). The principle of the arc system resides in its angular-independent aiming characteristic. Once the position of the arc on the frame is fixed, the locus of positions of the tool-holder describe part of a sphere, such that when the tool is set at the zero-offset position with respect to the tool-holder, the tip of the tool is exactly at the center of the sphere. By properly setting the position of the arc with respect to the frame so that the center of the sphere is exactly at the point of interest (the target), the neurosurgical tool will always point towards this target regardless of where it is attached on the arc<sup>3</sup>.

## 1.3 Conventional imaging modalities for thalamotomy and pallidotomy

At the MNI/H, the standard procedure for performing stereotactic localization of the targets makes use of multimodality imaging, including ventriculography (Figure 2), computed tomography (CT), and MRI scans. Even though landmarks such as the mid-plane (the sagittal cut between the two hemispheres) and the AC-PC plane<sup>†</sup> can be easily localized on ventriculograms, the positions of the target structures relative to such landmarks are not necessarily constant between patients, chiefly because of the variable size of the third ventricle.

Other imaging modalities such as (CT) and MRI also have shortcomings for this task. The structures of interest consist of white and/or gray matter. CT scans show very little contrast between white and gray matter. MRI, on the other hand can easily differentiate between white and gray matter, but cannot distinguish between two functionally distinct structures within gray matter, such as the Vim and Gpm. MRI is nevertheless the modality which provides the most information on the anatomy of the thalamus and its neighboring structures.

## 1.4 Stereotactic neurosurgical tools

The traditional approach in addressing this inter-patient variability has employed physiological verification of the position of target structures with respect to the stereotactic frame coordinate system by electrically stimulating the basal ganglia. A stimulating electrode is inserted into the patient's brain through the same drill-hole used for the injection of the ventriculography contrast agent. The stimulator consists of a small conducting wire inside a long metallic shaft. The wire is attached at one extremity to a screw which controls the extent of its protrusion from the tip of the shaft. The stimulator currently used at the MNI/H extends a maximum of 14 mm, obliquely from the shaft (Figure 3).

The neurosurgeon stimulates various regions of the thalamus and of the internal capsule (an important white matter structure which must be avoided during the ablation procedure) while observing sensory, motor, or visual responses from the patient<sup>2</sup>.

<sup>†</sup> The AC-PC plane contains the line between the anterior and posterior commissure (AC and PC) points and is perpendicular to the plane between the two hemispheres (the mid-plane).

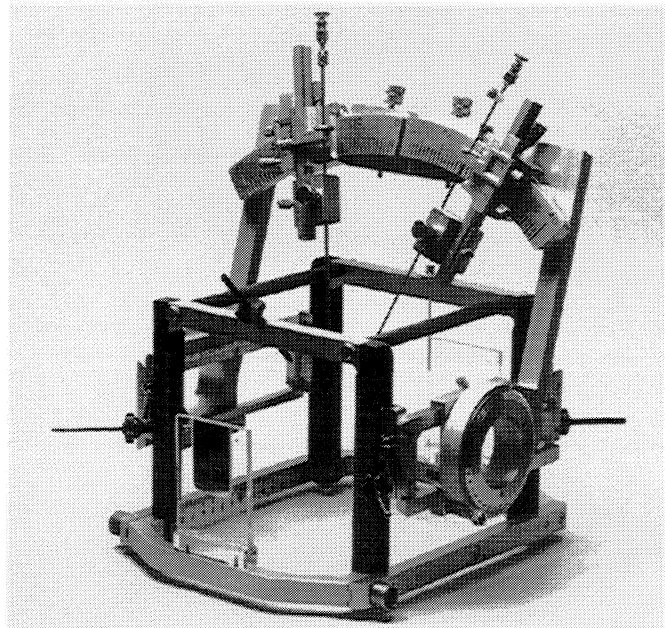


**Figure 1.** Arc system mounted on the stereotactic frame. Two biopsy needles are attached to the arc system installed on the frame.

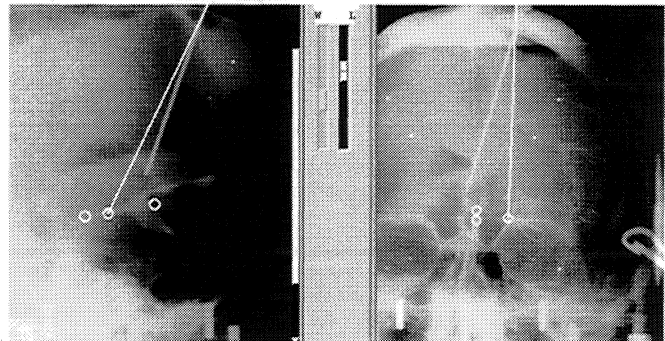


**Figure 2.** Ventriculograms. Lateral (left) and antero-posterior (right) ventriculograms with the AC, PC, and target points identified.

The information obtained from the electrical stimulation allows the neurosurgeon to determine the position of the target relative to the frame coordinate system with acceptable precision. Once sufficient information about the position of the important deep brain structures has been obtained, the surgeon can proceed to lesion the Vim or the Gpm.

At the MNI/H, the lesions are created using a leukotome, which consists of a narrow metallic wire protruding from a shaft (similar to the stimulator) so that it forms a loop which acts like a knife when the tool is rotated around its axis (Figure 3). Once again, a screw at the other extremity of the shaft controls the extent of the loop. The leukotome extends to a maximum distance of 7 mm from the shaft. The main advantage of the leukotome over other tools resides in its ability to create tailored lesions conforming to the shape of the target structure. While other methods are usually limited to spherical lesions, the leukotome allows for pre-defined lesions that can be geometrically adapted to the target volume to be excised. Custom lesion shapes can be achieved by varying the extension of the wire loop as the tool is rotated.

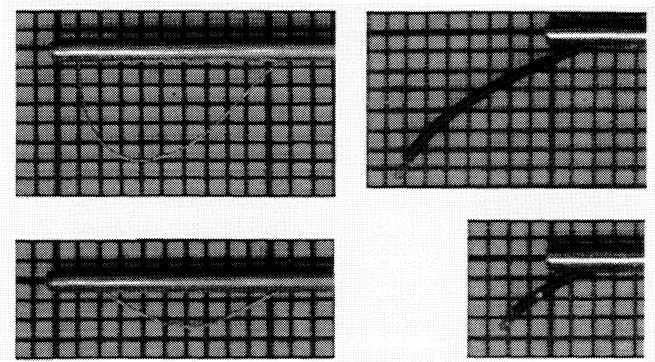


**Figure 3.** Optical scans of the leukotome (left) and the stimulator with two different protrusion settings.

Even though the conventional techniques described have been generally effective, the standard imaging modalities have not proven amenable to distinguishing these functionally different deep brain structures. This shortcoming inherently precludes the visualization of the patient-specific geometry of the basal ganglia, and their three-dimensional (3D) relationship with the intra-operative surgical tools. In order to provide interactive visual feedback to the neurosurgeon and to increase the accuracy of target localization, an intra-operative visualization platform has been designed and developed.

## 2. MATERIALS AND METHODS

### 2.1 Atlases and automatic labeling of deep brain structures

At present, the only references available to the clinician for localizing lesion targets during the operation are atlases of the anatomy of the deep brain<sup>4</sup>. These atlas structures will obviously differ in size, and sometimes in geometry, from those of any given patient's brain. In addition, the orientation of the patient's brain with respect to the slices presented in the atlas as well as the trajectory of the neurosurgical tools with respect to the structures described in the atlas are difficult to appreciate. Since no currently available imaging modality provides enough contrast between target structures, the solution implemented here was to enhance the information already available from routine MRI scans. The aim was to incorporate the precise contours of an anatomical atlas of the deep brain with an individual patient's MRI scan. It was hence desirable for this atlas to be volumetric, deformable, and easily orientable with respect to the patient's brain.

The Schaltenbrand and Wahren atlas is one of the principal anatomical references for neurosurgeons performing thalamotomies and pallidotomies<sup>5</sup>. This book gathers together many different data sets, three of which are of interest: the coronal (plates 35-40), sagittal (plates 41-51) and transverse (plates 52-57) cryogenic slices of a human cadaver's brain\*. Each of these three data sets consists of a series of micro-thin cryogenic slices which are stained to discriminate between structures presenting different cyto-architectures. The slices are not necessarily contiguous in space; each slice is separated from the next by a distance varying between 0.5 mm and 3 mm. Photographs of these slices are then taken under constant geometry. The outlines of the anatomical regions are drawn on acetate (transparency) sheets overlaid on top of photographs of these slices (Figure 4).

The objective was to create an easily deformable volumetric atlas from such an atlas composed of two-dimensional (2D) slices with varying inter-slice separations. Since the extent of the structures in the transverse (axial) plane was larger than in the other planes, the transverse series (from the right hemisphere) were used. In this series, about one hundred structures are outlined. The construction of the volumetric atlas was limited to sixteen regions which are of interest to clinicians in

\* The sagittal and axial sets come respectively from the left and right hemispheres of the same brain (cadaver brain number LXXVIII). The coronal set comes from another brain (LXVIII).



any individual MRI. This model MRI had been created from an average of 27 T1-weighted volumetric MRI scans, collected over a period of several months. These images were registered (to eliminate inter-scan motion) and averaged together. Since the signal-to-noise ratio (SNR) in the data set is inversely proportional to the square root of the number of acquisitions, this data set (called the “Super-brain” because of its low noise characteristics) has an SNR about 5.1 times higher than one obtained with a standard volumetric acquisition using the same imaging protocol (Figure 5).

Thin-plate spline 3D interpolation<sup>9</sup> allows a smooth non-linear deformation from a volumetric data set to another, based on a set of homologous point pairs. In this case, each pair of points consisted of corresponding anatomical landmarks—one point from the model MRI data set and the other from the atlas. The manual tagging of the 250 corresponding landmarks was performed by a neuroanatomist (Figure 6). The thin-plate spline interpolation forces all 250 points from the atlas to be mapped onto their corresponding points on the model MRI, while the regions in between the points are smoothly warped into the new space. The strategy was to manually identify the point pairs once only, so that the atlas would be definitively mapped onto this model MRI. Once this was achieved, the non-linear transformation from the model MRI to any patient’s MRI was automatically computed using the ANIMAL algorithm. Since the atlas is already in correspondence with the MRI model space (from the manual registration), this last transformation can be applied to the atlas in order to bring it onto the patient’s MRI. Thus the steps involved in registering the atlas with the patient’s MRI are:

- Manual tagging of corresponding landmarks on the atlas and on a model MRI (performed once only by a neuroanatomist)
- Deformation of the atlas onto the model MRI using thin-plate spline interpolation from the set of corresponding landmarks (also performed only once)
- Automatic calculation of the transformation from model MRI space to each patient’s MRI using ANIMAL
- Deformation of the model-space atlas onto the patient’s MRI space using the same non-linear transformation

### 2.3 A visualization platform

The IGNS lab at the MNI has created a visualization platform, VIPER (Visual Integration Platform for Enhanced Reality), for clinical applications. It is coded in C++ using two well-known and widely used libraries, namely Motif (Open Software Foundation) for the graphical user interface (GUI), and OpenGL (Silicon Graphics Inc., Mountain View, CA) for rendering-related tasks.

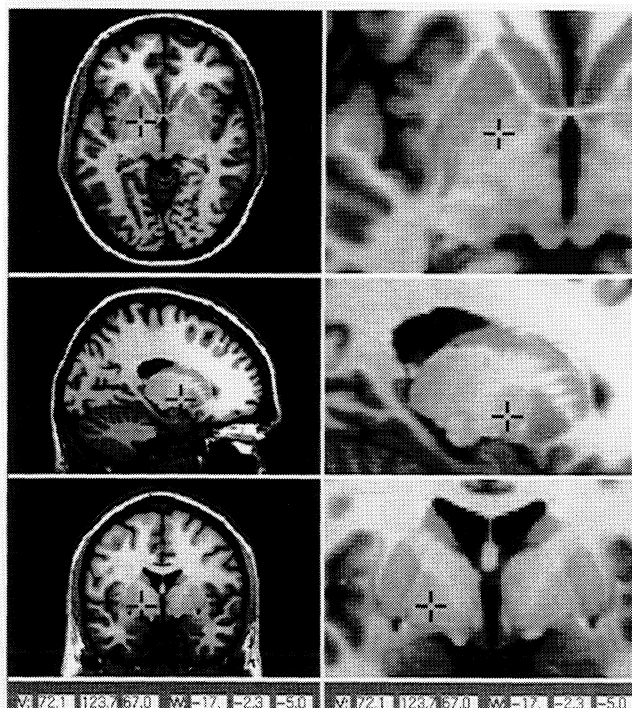


**Figure 5.** The MRI model data set: axial, sagittal, and coronal cuts (top to bottom), and detail (right series).

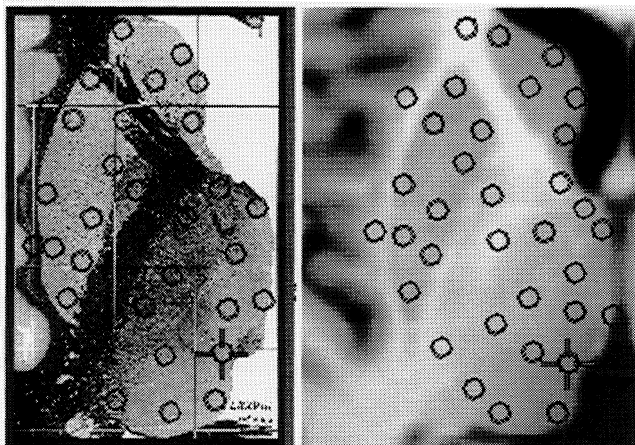


**Figure 6.** Corresponding tag points between the atlas (left) and the MRI model.

### 2.3.1 2D and 3D views

The system is capable of superimposing (or merging) images from multiple modalities such as MRI, CT, atlas slices, functional and metabolic scans. The opacity (or relative blending) of the slices as well as the window/level and color-map for every individual scan can be adjusted independently<sup>13</sup>. Apart from the standard tri-planar views, two oblique orientations are also available. The “gun-view” orientation shows the plane perpendicular to a virtual needle that would be inserted in the patient’s head at some given declination and azimuthal angle. The other view, called the “ultrasound-view”, shows the plane containing the trajectory of the needle. In this parallel orientation, the declination and azimuth angles define a line that lies in the cutting plane, and this “ultrasound-view” plane is not fully defined until the twist angle is provided by a readout on the surgical needle.

In addition, objects such as the vectorized structures of the Schaltenbrand atlas can be displayed as surface renderings, again with independent colors and opacities which is helpful, for example, in visualizing the thalamic nodes inside a semi-transparent thalamus (see Figure 7). The 2D and 3D windows are in the same coordinate system, and the x-, y-, and z-axes

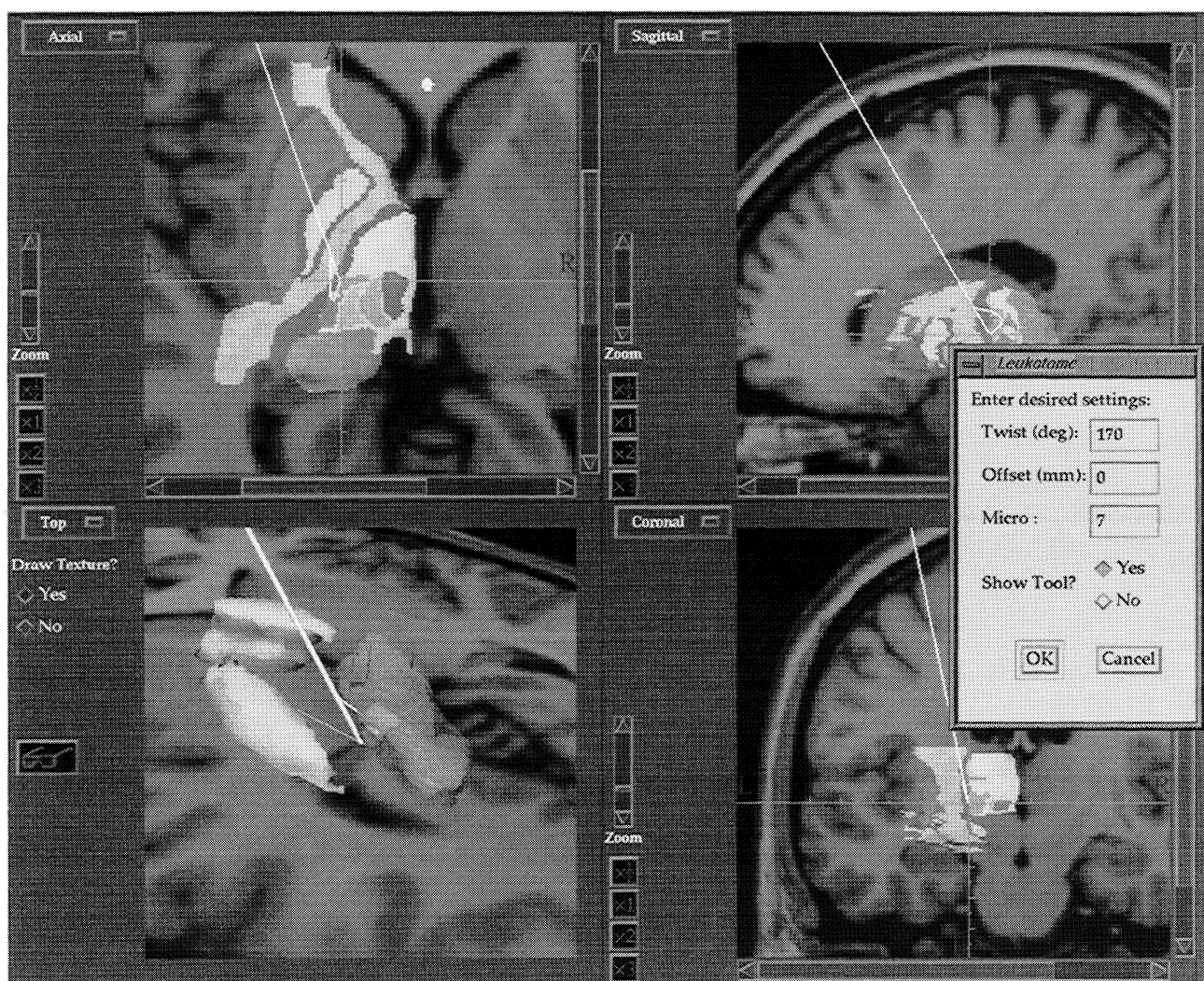


**Figure 7.** The visualization platform. In the three 2-D views the atlas has been superimposed on the super-brain model. Projections of the leukotome onto the three standard planes can be seen in white. In the bottom left (3-D) view, surface-renderings of the putamen, caudate, thalamus (semi-transparent) and Vim node can be seen, along with the leukotome and a texture map of the current axial slice for added anatomical context.

displayed in the 3D window are correlated to the cross-hairs defining the point of interest in the 2D windows. In the 3D view, the objects can be manipulated interactively, enabling the user to rotate, translate, and zoom as desired.

### 2.3.2 Virtual neurosurgical tools

The stimulator and the leukotome were optically scanned on a HP ScanJet IIcx (see Figure 3). The position of the

stimulator electrode was measured for all fourteen possible settings (or extents) of the tip. For the leukotome, samples of the distance between the metallic wire and the shaft of the leukotome were taken every millimeter on all ten millimeters across which the wire can protrude along the shaft. This was done for all seven different settings (protrusions) of the leukotome loop. These values were entered into the software, so that the neurosurgical tools could be drawn at all their possible settings in the 2D and 3D windows. The position of the leukotome with respect to the co-registered atlas and MRI data set is fully controllable by the user. The position of the target point (the point where the tip of the leukotome should be) and the two angles of entry (declination and azimuth) must be specified first. These parameters can be given either in the native MRI coordinate system, or more commonly, in the stereotactic frame coordinate system. Note that in the standard 2D views an orthogonal projection of the complete tool is drawn, rather than simply the points where the shaft intersects the 2D (sagittal, coronal, or axial) plane.

### 2.3.3 Stereoscopic Viewing

Many of the monocular depth cues such as perspective, shading, occultation, and texture have been incorporated into the 3D view. One of the strongest short-range depth cues, however, is stereopsis which relies on binocular vision<sup>11</sup>. In order to make full use of the human visual system's depth perception capabilities, the VIPER platform is capable of displaying a pair of images in stereo. These images are rendered from two slightly different viewpoints, simulating the left- and right-eye views of the 3D objects (Figure 8). The images are drawn on the computer monitor in a time-multiplexed fashion, such that the right and left views are alternated. Stereoscopic viewing is then enabled using a pair of CrystalEyes shuttered goggles (StereoGraphics Corporation, San Rafael, CA) synchronized through an infra-red emitter to the monitor's refresh rate, such that the right- and left-eye images are presented at the appropriate times<sup>12</sup>. In the stereoscopic mode, the user is still able to manipulate the 3D objects, and the control panel for the leukotome is also available, so that it may still be rotated and translated as in the monoscopic mode.

## 2.4 Lesion modeling

In addition to the visualization platform described, a small graphical interface has been created which allows the surgeon to define volumetric lesions in a user-friendly manner. The graphical interface is presented in the shape of a dart-board divided into sixteen sectors (Figure 9). Each of these sectors is divided into seven concentric parts, corresponding to the seven possible settings of the leukotome, giving a total of 112 (7x16) small regions. The surgical protocol allows the leukotome three degrees of freedom (after a particular trajectory has been set): changing the insertion depth (offset) with respect to the target point; rotating about the axis of the shaft; and changing the protrusion of the wire loop. Consequently, the software allows for three different depths, as well as the 112 regions described above. The user highlights the protrusion setting desired at each of the 16 sectors at each depth. Once the virtual lesion is created, it can be visualized on the VIPER platform either as a tomographic volume or as a 3D surface-rendered object. It can then be compared with the atlas to ensure that no part of this target lesion overlaps with structures that should not be excised (Figure 10). The 3D view gives more insight on the global extent of the lesion and on the shape of the lesion with respect to the target. By showing the leukotome in the 3D view, the user can rotate the tool to a region (sector) where the lesion extent is inappropriate, find a better setting for that

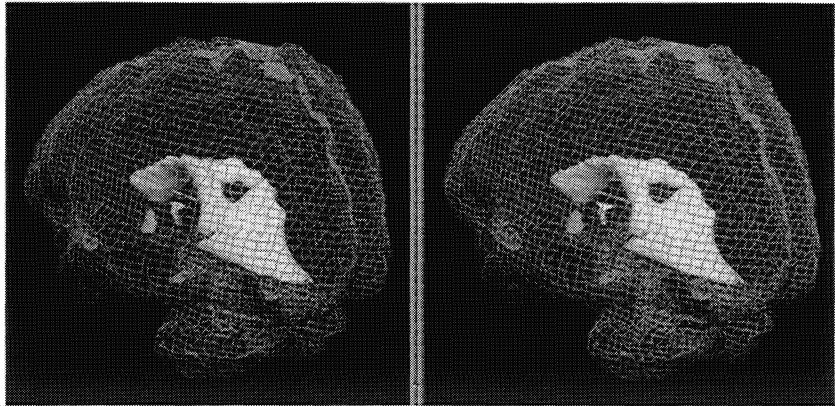


**Figure 8.** Stereoscopic image pair showing a surface-rendering of a cerebral ventricle inside a mesh model of the cortex. The images are arranged here for cross-eyed viewing, but in practice they are superimposed and displayed alternately.

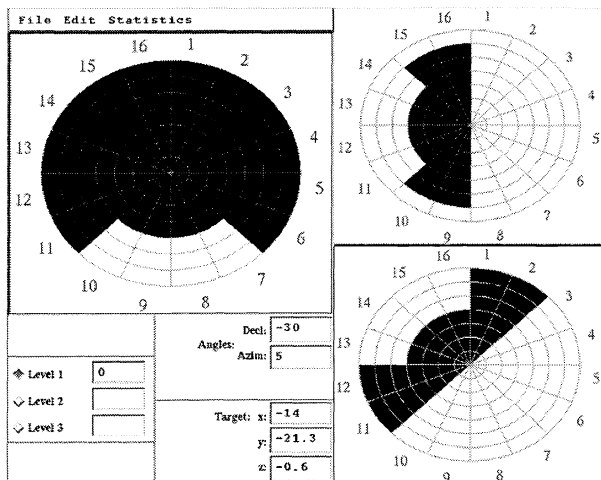


**Figure 9.** The lesion modeling graphical interface (left), along with two other examples of other possible excision maps.

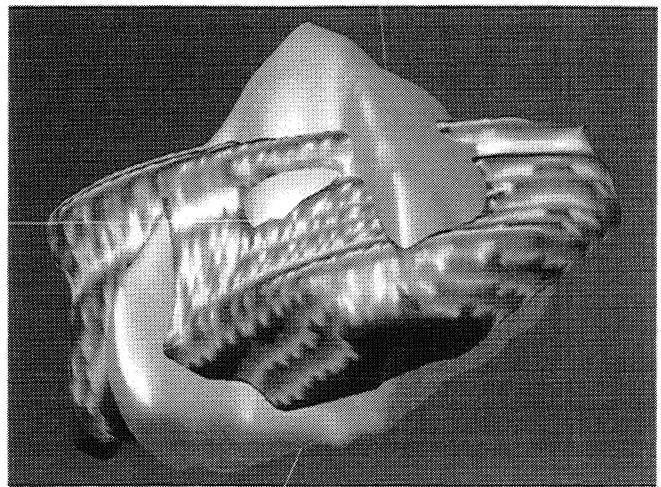


**Figure 10.** A 3D view of a virtual lesion (flat gray) of the Gpm (textured gray).

sector, and then update the shape of the virtual lesion. In fact, the clinician does not rely solely on the 3D view but also on standard tomographic views where the inspection is performed on a slice-by-slice basis in all three projections in order to make use of the detailed anatomical information provided by the MRI.

### 3. RESULTS AND DISCUSSION

At the time of this writing, 17 patients have undergone operations where this visualization platform has been used. At this stage, the platform is used as an investigational tool only, and always in conjunction with the standard procedures and tools for these operations (e.g., ventriculography, intra-operative x-rays, stimulation runs, etc.).

Although the clinical feedback has been positive, there remain a few drawbacks associated with the software. It is often quite difficult to characterize the overall accuracy and reproducibility (precision) of this type of system. Even though certain parts of the overall procedure have been well studied, a more conclusive and comprehensive characterization is for future consideration. Although the transformation of the native MRI into frame coordinates through identification of MRI-visible markers is accurate to within 1-1.5 mm (due to operator mis-measurement)<sup>14</sup>, the geometrical artifacts due to field inhomogeneity are highly dependent on the imaging parameters and can lead to distortions of up to 5 mm if no precautions are taken<sup>15</sup>. However, the overall accuracy of the deep-brain anatomical structures on a MRI acquired with a stereotactic frame can be considered to be on the order of 2 mm.

In a report describing the performance of the ANIMAL algorithm<sup>16</sup>, Collins *et al.* show a volumetric overlap and difference of better than 85% and less than 10%, respectively, for a few deep brain structures at the level of the ventricles and basal ganglia. This is on the order of intra-observer variability estimates of 87% and 5%, for manual 3D segmentation of the same structures. Since no impartial clinical measure of truth exists, the accuracy of the atlas-to-model tagging is not easy to evaluate. On the other hand, more than 250 point pairs were used to map only 16 structures between an atlas of cryogenic slices and a high-resolution low-noise MRI volume, by a trained neuroanatomist. Clinically speaking, if there is any doubt or ambiguity in the mind of the surgeon, a potential lesion can be thoroughly verified through the stimulation procedure. In fact cross-validation between stimulation results and computed atlas structures is the subject of on-going study.

The choice of the model MRI is a fundamental element in the success of all the steps necessary in warping the atlas to a patient's MRI. The quality of the manual tagging of the atlas and the performance of the ANIMAL algorithm depend strongly on this choice. One of the most important criteria is the SNR in the image. Lower noise in the model data set will result in a better non-linear fit and easier manual tagging. It is important to note that of the four steps in creating an individualized atlas, it is only the last two (which require no intervention from a specialist) which must be performed for every clinical case. In this regard the labor-intensive manual tagging of the atlas to the model brain has been performed once, and it is the computationally-expensive process of warping the model to the patient's MRI which is repeated.

The representation of the leukotome and stimulator in the 2D views as projections onto the standard orthogonal planes can be ambiguous, giving the impression that the tool lies in one of the orthogonal planes. This would cause a problem when using the leukotome since the projection of the wire loop may fall on a 2D cut of an anatomical structure, when it is not actually in contact with it. Simultaneous use of trajectory views and 3D surface models removes this ambiguity.

Indeed, the type of visual information that is available in the 2D display panels is often a limiting factor in a number of ways. The fact that only slices through the volume can be visualized rather than complete 3D structures forces the neurosurgeon to mentally extrapolate the extent of these structures outside of the slice, which is often challenging. It is particularly difficult to reconstruct the overall shape, size, and orientation of a region of the anatomy or of a lesion site in the brain. Finally it is also difficult to assemble different neighboring parts together in space and to imagine how they are spatially inter-related. It is in order to compensate for these inherent limitations of 2D visualization that 3D views have been developed, allowing more insight into the global geometry of objects of neurosurgical interest. In general, the 3D views have greatly facilitated the visualization of the operative tools with respect to the anatomical structures, since these tools are often rotated around axes that are already rotated with respect to the standard stereotactic frame axes.

#### 4. CONCLUSIONS

During a thalamotomy, two neurosurgical tools (the electrical stimulator and the leukotome) are inserted deep into the patient's brain. Since no craniotomy is performed during this operation, the neurosurgeon does not directly see the position of the tools with respect to anatomical structures. The neurosurgeon must mentally reconstruct both the geometry of the target structure and the position of the neurosurgical tools with respect to the anatomy. In the system described, the anatomy is already displayed either on 2D slices or in the 3D window as surface-rendered objects. The position and geometry of the neurosurgical tools with respect to these deep brain structures may also be displayed on the 2D slices, as well as in the 3D window. While the conventional tools provide sufficient information and precision to allow for thalamotomies and pallidotomies to be performed, the present tools enhance the neurosurgeon's ability to reconstruct the geometry of critical structures in 3D space. In this sense these tools can facilitate the work of neurosurgeons, providing them with most of the necessary geometrical information within acceptable accuracy requirements.

#### 5. ACKNOWLEDGEMENTS

The authors wish to thank Dr. Noor Kabani, whose help in tagging the anatomical atlas to the model MRI was instrumental to this project, and also Mr. Roch Comeau for many fruitful discussions and his support in all aspects of this project. This work was supported by operating grants from the Medical Research Council (A.F.S., A.C.E., T.M.P.) and the Natural Sciences and Engineering Research Council (A.C.E., T.M.P.) of Canada. P.S.-J., D.C., and R.K. were supported by NSERC post-graduate scholarships.

#### 6. REFERENCES

1. A. E. Walker, *Classification of movement disorders*, Chapter 33, pp. 515-521, Georg Thieme Verlag, 1982.
2. G. Bertrand, H. Jasper, A. Wong, and G. Matthews, "Microelectrode recording during stereotactic surgery", *Clinical Neurosurgery*, **16**, pp. 328-355, 1969.
3. A. Olivier and G. Bertrand, "Stereotaxic device for percutaneous twist-drill insertion of depth electrodes and for brain biopsy", *Journal of Neurosurgery*, **56**, pp. 307-308, 1982.
4. J. Talairach, M. David, P. Tournoux, H. Corredor, and T. Kvasina. *Atlas d'anatomie stéréotaxique*. Masson et Cie., Paris, 1957.
5. G. Schaltenbrand and P. Wahren, *Introduction to stereotaxis with an atlas of the human brain (Volume II)*, Georg Thieme Verlag, Stuttgart, 1977.
6. D. L. Collins, W. Dai, T. S. Marrett, and A. C. Evans, "Three-dimensional non-linear warping of a computerized volume-of-interest brain atlas for morphometric analysis", *Information Processing in Medical Imaging (poster session)*, Wye, UK, July 1991.
7. D. L. Collins, *3D model-based segmentation of individual brain structures from magnetic resonance imaging data*, Ph.D. thesis, McGill University, Montreal, Canada, 1994.
8. D. L. Collins, T. M. Peters, and A. C. Evans, "An automated 3D non-linear image deformation procedure for determination of gross morphometric variability in the human brain", *Proceedings of the Third Conference on Visualization in Biomedical Computing*, Richard A. Robb (ed.), **2359**, pp. 180-190, SPIE, Rochester, MN, 1994.

9. F. L. Bookstein, "Principal warps: Thin-plane splines and the decomposition of deformations", *IEEE Transactions on Pattern Analysis and Machine Intelligence, PAMI-11*, **6**, pp. 567-585, 1989.
10. C. J. Holmes, R. D. Hoge, D. L. Collins, R. Woods, A. W. Toga, and A. C. Evans, "Enhancement of magnetic resonance imaging using registration for signal averaging", *Journal of Computer Assisted Tomography* (in press).
11. R. Patterson, "Human stereopsis", *Human Factors*, **34(6)**, pp. 669-692, 1992.
12. B. L. K. Davey, R. M. Comeau, P. Munger, L.J. Pisani, D. Lacerte, A. Olivier, and T. M. Peters, "Multimodality interactive stereoscopic image-guided neurosurgery", *Proceedings of the Third Conference on Visualization in Biomedical Computing*, Richard A. Robb (ed.), **2359**, pp. 180-190, SPIE, Rochester, MN, 1994.
13. R. Kasrai, P. St-Jean, M. C. Preul, S. Narayanan, D. L. Arnold, and T. M. Peters, "Multimodality image visualization for image-guided neurosurgery", *Proceedings of the 43<sup>rd</sup> Annual Scientific Meeting of the Canadian Organization of Medical Physicists*, pp. 137-139, Charlottetown, Canada, 1997.
14. P. Munger, *Accuracy considerations in MR image-guided neurosurgery*, M.Sc. thesis, McGill University, Montreal, Canada, November 1994.
15. A. Gauvin, *Geometrical distortion of magnetic resonance images*, M.Sc. thesis, McGill University, Montreal, Canada, May 1992.
16. D. L. Collins, C. J. Holmes, T. M. Peters, and A. C. Evans, "Automatic 3-D model-based neuroanatomical segmentation", *Human Brain Mapping*, **3**, pp. 190-208, 1995.
17. D. Clonda, P. St-Jean, A. F. Sadikot, T. M. Peters, and A. C. Evans, "Automatic labeling of the patient's brain with a subcortical atlas in image-guided neurosurgery", *Proceedings of the 43<sup>rd</sup> Annual Scientific Meeting of the Canadian Organization of Medical Physicists*, pp. 209-211, Charlottetown, Canada, 1997.